NASA-CR-192189

Optimal Guidance Law Development for an Advanced Launch System

Interim Progress Report
1 December 1990 - 15 June 1991

June 1991

Research Supported by NASA Langley Research Center

NASA Grant No. NAG-1-939

Principal Investigators: Anthony J. Calise & Dewey H. Hodges

Research Assistant: Martin S. Leung & Robert R. Bless

NASA Grant Monitor: Daniel D. Moerder

Georgia Institute of Technology
School of Aerospace Engineering
Atlanta, GA 30332-0150

Summary

Following the previous report, the proposed investigation on a Matched Asymptotic Expansion (MAE) method was carried out. It was concluded that the method of MAE is not applicable to launch vehicle ascent trajectory optimization due to a lack of a suitable stretched variable. More work was done on the earlier regular perturbation approach using a piecewise analytic zeroth order solution to generate a more accurate approximation. In the meantime, a singular perturbation approach using manifold theory is also under current investigated

Work on a general computational environment based on the use of MACSYMA and the weak Hamiltonian finite element method continued during this period. This methodology is capable of the solution of a large class of optimal control problems. This part of the work continued until the departure of Dr. Robert R. Bless, who was supported under the grant as a Graduate Research Assistant at Georgia Tech. The first version of his computer code is now complete. A NASA contractor report (CR), based on Dr. Bless' Ph.D. Dissertation [1] is presently in press. It contains the details of the general code as well as sample input and output. These details are not repeated herein. Work has continued since his departure to more fully understand the accuracy and limitations of the method and to adapt Dr. Bless' code to use Mathematica which is available on a wider variety of computers than MACSYMA.

Table of Contents

1. Research Accomplishments

1.1 Matched Asymptotic Expansion (MAE) Investigation

The MAE approach was first investigated to handle the launch vehicle atmospheric flight phase where the earlier regular perturbation approach did not produce satisfactory results. The essence of the MAE approach is outlined below.

We first evaluate the outer solution which corresponds to a propulsion dominant phase of flight. This part of the solution is just our zeroth order solution in the earlier regular perturbation approach [12]. Next, we formulate the inner solution which corresponds to an aerodynamic force dominant phase. This part of the solution has been developed in [9] where the analytic solutions involve elliptical integrals of the first and second kind. Finally, a composite solution is formed by joining the outer and inner parts with the extraction of the common part using the matching conditions (see [10] and [11] for details).

First of all, we non-dimensionalize and rewrite the dynamics as:

$$\frac{d\hat{V}}{d\hat{t}} = \frac{\hat{T}_{vac}}{\hat{m}}\cos\alpha - \frac{\hat{p}_i e^{-\hat{h}/\varepsilon}}{\hat{m}}\cos\alpha - \frac{\hat{\rho}_i \hat{V}^2 (k_0 + k_1\alpha + k_2\alpha^2 + \delta K)e^{-\hat{h}/\varepsilon}}{\varepsilon 2\hat{m}} - \sin\gamma + \delta\left\{1 - \frac{1}{(1+\hat{h})^2}\right\}\sin\gamma \qquad 1)$$

$$\hat{V}\frac{d\gamma}{d\hat{t}} = \frac{\hat{T}_{vac}}{\hat{m}}\sin\alpha - \frac{\hat{p}_i e^{-\hat{h}/\varepsilon}}{\hat{m}}\sin\alpha + \frac{\hat{\rho}_i \hat{V}^2 (\eta_0 + \eta_1\alpha + \delta N)e^{-\hat{h}/\varepsilon}}{\varepsilon 2\hat{m}} - \cos\gamma + \delta\left\{(1 - \frac{1}{(1+\hat{h})^2})\cos\gamma + \frac{\hat{V}^2\cos\gamma}{1+\hat{h}}\right\} \qquad 2)$$

$$\frac{d\hat{h}}{d\hat{t}} = \hat{V}\sin\gamma \qquad 3)$$

$$\frac{d\hat{m}}{d\hat{t}} = -\hat{c} \qquad 4)$$

where

$$\varepsilon = \frac{1}{\beta r_i} \qquad \hat{c} = \frac{c}{m_i\sqrt{g_i / r_i}} \qquad \hat{p}_i = \frac{p_i A_e}{m_i g_i}$$

$$\hat{h} = \frac{h}{r_i} \qquad \hat{T}_{vac} = \frac{T_{vac}}{m_i g_i} \qquad \hat{m} = \frac{m}{m_i}$$

$$\hat{V} = \frac{V}{\sqrt{r_i g_i}} \qquad \hat{\rho}_i = \frac{\rho_i S}{\beta m_i} \qquad \hat{t} = \frac{t}{\sqrt{r_i / g_i}}$$

$$h = r - r_i \qquad \rho = \rho_i e^{-\beta(h-h_i)} \qquad p = \frac{\rho_i g_i}{\beta} e^{-\beta h}$$

$$C_D(\alpha,M) = k_0 + k_1\alpha + k_2\alpha^2 + \delta K(\alpha,M) \qquad C_L(\alpha,M) = \eta_0 + \eta_1\alpha + \delta N(\alpha,M)$$

The notation of the variables are self-explanatory. The hatted variables are non-dimensional and the subscript i stands for initial value of the variables. Here ε is a small physical parameter whereas δ is a bookkeeping perturbation parameter with a nominal value of one. We are actually using a combination of singular and regular perturbation expansions. Setting ε to zero, we retrieve the zeroth order outer dynamics (no aerodynamic forces). On the other hand, introducing the stretched variables $t = \hat{t}/\varepsilon$, $h = \hat{h}/\varepsilon$ and setting ε to zero we obtain the zeroth order inner dynamics (no thrust terms). The atmospheric pressure and the Mach number dependency of the aerodynamics data will be introduced in the first order correction which will subsequently involve solving a set of non-homogeneous linear O. D. E's. The advantage of this approach over our earlier perturbation approach lies in the fact that we are now able to introduce aerodynamic forces in our zeroth order formulation.

Our first attempt was to evaluate the composite zeroth order solution using the existent results in [9,12] by solving a set of 21 nonlinear algebraic equations. However, we were not able to find a solution The problem is not due to numerical difficulties but lies in the flaws of our MAE arguments. From the optimal solution using BNDSCO we determined that magnitude of the aerodynamic forces is less than 15% of the thrust over the whole trajectory, which means there is never a flight phase where the aerodynamic forces dominate over the propulsive force. However, the magnitude of the aerodynamics forces is largely determined by the dynamic pressure profile. The aerodynamic forces increases as dynamic pressure initially builds up due to gain in velocity. As the launch vehicle rises in altitude, the drop in air density outweighs the gain in velocity and the dynamic pressure decreases. This phenomenon indicates that we need two different regions (2 pairs of outer and inner solutions) to formulate our whole trajectory (see figure 1). We also need a new independent variable such that if it is set to the right and left hand side limits, the two respective outer solutions are obtained. Clearly, altitude is not the suitable candidate because we can only retrieve the right hand side of our solution as $h \to \infty$.

In a nutshell, we conclude that the traditional (using altitude as the stretched variable) MAE approach which has found success in aero-assisted orbital transfer application is not applicable in a straight forward manner to the ascent trajectory launch vehicle problem. Further research is needed to identify a more suitable independent variable. Rather than pursue this line of investigation, we decided to return to our earlier regular perturbation study, and to investigate a singular perturbation approach based on a slow manifold concept.

1.2 A Modified Regular Perturbation Approach

An idea to extend the earlier regular perturbation method into the atmospheric flight phase is through a finite element approach. Since we cannot find a complete analytic zeroth order solution that incorporates the aerodynamic effects, our approach is to improve accuracy with minimal increase in computational complexity. Using several pieces of simple solutions instead one complete and complicated solution, we are able to improve the zeroth order solution so that it accounts for the aerodynamic effects.

From our earlier study, the state dynamics can be fairly represented by those of a flat Earth no atmosphere approximation. However, this is not true of the costate dynamics. If we use the previous approximation, we will end up with (in a rectangular coordinate system):

$$\dot{v} = \frac{T_{vac}\sin\beta}{m_i - ct} - g_e + \varepsilon\left\{\frac{-A_e p\sin\beta - D\sin\gamma + L\cos\gamma}{m_i - ct} + (g_e - \frac{\mu_e}{r^2})\right\} \quad 5)$$

$$\dot{u} = \frac{T_{vac}\cos\beta}{m_i - ct} + \varepsilon\left\{\frac{-A_e p\cos\beta - D\cos\gamma - L\sin\gamma}{m_i - ct} - \frac{uv}{r}\right\} \quad 6)$$

$$\dot{r} = v \quad 7)$$

$$\dot{\lambda}_v = -\lambda_r - \varepsilon(\lambda_v \frac{\partial\dot{v}}{\partial v} + \lambda_u \frac{\partial\dot{u}}{\partial v}) \quad 8)$$

$$\dot{\lambda}_u = -\varepsilon(\lambda_v \frac{\partial\dot{v}}{\partial u} + \lambda_u \frac{\partial\dot{u}}{\partial u}) \quad 9)$$

$$\dot{\lambda}_r = -\varepsilon(\lambda_v \frac{\partial\dot{v}}{\partial r} + \lambda_u \frac{\partial\dot{u}}{\partial r}) \quad 10)$$

The approximate set of zeroth order dynamics are especially poor in λ_u and λ_r because both derivatives become zero to zeroth order in ε. Consequently, they produce large forcing function

terms (in L_2-norm sense) in the first order correction dynamics which may cause divergence of our corrected results. The easy way to decrease these large error magnitudes is to represent the λ_u and λ_r with linear function such that

$$\dot{\lambda}_u = p_u - \varepsilon(\lambda_v \frac{\partial \dot{v}}{\partial u} + \lambda_u \frac{\partial \dot{u}}{\partial u} + p_u) \quad 11)$$

$$\dot{\lambda}_r = p_r - \varepsilon(\lambda_v \frac{\partial \dot{v}}{\partial u} + \lambda_u \frac{\partial \dot{u}}{\partial u} + p_r) \quad 12)$$

and p_u, p_r are constants to be determined by other means. The optimal control of the zeroth order problem is now governed by a bilinear tangent law.

The constants p_u and p_r are evaluated using collocation method [13]. We approximate the solution with pre-specified functions, in this case first order polynomials. Constraining the solution such that it is continuous at the node and satisfies the original dynamics at the mid point of each segment determines the unknown coefficients of the polynomials. Mathematically, these constraints are formulated as follows:

$$p_u = \frac{\lambda_{u2} - \lambda_{u1}}{t_2 - t_1} = \left\{ -\lambda_v \frac{\partial \dot{v}}{\partial u} - \lambda_u \frac{\partial \dot{u}}{\partial u} \right\}\Big|_{t=\frac{t_1+t_2}{2};\ v=\frac{v_1+v_2}{2};\ \ldots;\ \lambda_r=\frac{\lambda_{r1}+\lambda_{r2}}{2}} \quad 13)$$

$$p_r = \frac{\lambda_{r2} - \lambda_{r1}}{t_2 - t_1} = \left\{ -\lambda_v \frac{\partial \dot{v}}{\partial r} - \lambda_u \frac{\partial \dot{u}}{\partial r} \right\}\Big|_{t=\frac{t_1+t_2}{2};\ v=\frac{v_1+v_2}{2};\ \ldots;\ \lambda_r=\frac{\lambda_{r1}+\lambda_{r2}}{2}} \quad 14)$$

The unknowns to be solved are the nodal values (subscript 1, 2) of the interpolated variables. However, for this linear function case, we simply equate the unknowns p_u and p_r with the averages, ie.

$$p_u = \frac{\lambda_{u2} - \lambda_{u1}}{t_2 - t_1} = -\frac{1}{2}\left\{ (\lambda_v \frac{\partial \dot{v}}{\partial u} + \lambda_u \frac{\partial \dot{u}}{\partial u})\Big|_{t_1;\ v_1;\ldots;\ \lambda_{r1}} + (\lambda_v \frac{\partial \dot{v}}{\partial u} + \lambda_u \frac{\partial \dot{u}}{\partial u})\Big|_{t_2;\ v_2;\ldots;\ \lambda_{r2}} \right\} \quad 15)$$

$$p_r = \frac{\lambda_{r2} - \lambda_{r1}}{t_2 - t_1} = -\frac{1}{2}\left\{ (\lambda_v \frac{\partial \dot{v}}{\partial r} + \lambda_u \frac{\partial \dot{u}}{\partial r})\Big|_{t_1;\ v_1;\ldots;\ \lambda_{r1}} + (\lambda_v \frac{\partial \dot{v}}{\partial r} + \lambda_u \frac{\partial \dot{u}}{\partial r})\Big|_{t_2;\ v_2;\ldots;\ \lambda_{r2}} \right\} \quad 16)$$

Figures 2 - 8 show an open loop 4-piece zeroth order solution segmented at 30s, 60s, 90s. In our present formulation, we also treat λ_v as a linear function with the unknown p_v. The first 3 segments are computed using collocation method described above, and the last segment uses a flat Earth approximation ($p_u = p_r = 0$). As a comparison, the costate profiles (figures 6 - 8) of the

earlier 1-piece zeroth order solution and the optimal solution (see Errata) are also plotted. We can clearly observe the significant improvements of this modification.

The new analytic expressions of v, u, h are given below:

$$v(t) = \frac{T_{vac}D}{c}\left\{\frac{\varsigma+\Delta}{\sqrt{1+\Delta^2}}\sinh^{-1}[\tan(\theta+\omega)] - \sinh^{-1}(\tan\theta)\right\}\Bigg|_{\theta(t_i)}^{\theta(t)} - g_e(t-t_i) + v_i \qquad 17)$$

$$u(t) = \frac{T_{vac}E}{c}\left\{\frac{1+\Delta\xi}{\sqrt{1+\Delta^2}}\sinh^{-1}[\tan(\theta+\omega)] - \xi\sinh^{-1}(\tan\theta)\right\}\Bigg|_{\theta(t_i)}^{\theta(t)} + u_i \qquad 18)$$

$$\begin{aligned} h(t) = &-\frac{T_{vac}DC}{cA}\left\{(\Delta-\tan\theta)[\frac{\varsigma+\Delta}{\sqrt{1+\Delta^2}}\sinh^{-1}[\tan(\theta+\omega)] - \sinh^{-1}(\tan\theta)\right\}\Bigg|_{\theta(t_i)}^{\theta(t)} \\ &-(t-t_i)\frac{T_{vac}D}{c}\left\{\frac{\varsigma+\Delta}{\sqrt{1+\Delta^2}}\sinh^{-1}[\tan(\theta+\omega)] - \sinh^{-1}(\tan\theta)\right\}\Bigg|_{\theta(t_i)} \\ &-\frac{1}{2}g_e(t-t_i)^2 + v_i(t-t_i) + h_i \end{aligned} \qquad 19)$$

where

$$A = \sqrt{p_v^2 + p_u^2} \qquad B = \frac{c_v p_v + c_u p_u}{A} \qquad C = \sqrt{c_v^2 + c_u^2 - B^2}$$

$$D = \frac{p_v}{A} \qquad \Delta = \frac{m_i A + cB}{cC} \qquad \varsigma = \frac{c_v A - p_v B}{p_v C}$$

$$\tan\theta = \frac{At+B}{C} \qquad \xi = \frac{p_u C}{c_u A - p_u B} \qquad E = \frac{c_u A - p_u B}{AC}$$

$$\omega = \begin{cases} \tan^{-1}(1/\Delta) & ;\ \Delta \geq 0 \\ \pi + \tan^{-1}(1/\Delta) & ;\ \Delta < 0 \end{cases}$$

The state transition matrix can be found by differentiating the above analytic expressions with respect to the initial values (c_v, c_u, c_r are the initial costate values). First order correction using the zeroth order solution above and the state transition matrix will be obtained in next progress report.

1.3 Singular Perturbation Approach Using Manifold Theory

In [15], we showed that a singular perturbation, using a 2-state model with mass and energy as slow variables, failed because the flight path angle dynamics are highly coupled with the slow variables at high flight path angle. However, if we use a more accurate 3-state model (mass,

energy and altitude), a chattering solution of flight path angle will be encountered. Our proposed research for the next reporting period is to attempt to use the Manifold condition [14]:

$$g = \varepsilon(\frac{\partial \phi}{\partial x} f + \frac{\partial \phi}{\partial t}) \tag{20}$$

where

$$\frac{dx}{dt} = f(x,z,t) \qquad \varepsilon \frac{dz}{dt} = g(x,z,t) \qquad z = \phi(\varepsilon, x, t)$$

to generate another zeroth order outer solution (slow manifold). Since we now include ε in our slow manifold (ϕ) formulation, the chattering effect is eliminated. Our first step is to demonstrate that we can compute an off-line slow manifold solution and perform an on-line boundary layer (inner solution) correction for the flight path angle dynamics. This will result in a nonlinear feedback control solution for the angle of attack (see below).

$$H = \hat{\lambda}_{Eo} \dot{E}(\hat{E}_o, \hat{h}_o, \hat{m}_o, \alpha) + \hat{\lambda}_{ho} \hat{V}_o \sin\gamma - \hat{\lambda}_{mo} k + \lambda_\gamma \dot{\gamma}(\hat{E}_o, \hat{h}_o, \hat{m}_o, \alpha) = 0 \tag{21}$$

$$H_\alpha = 0 \tag{22}$$

These two equations are used to determine α and λ_γ. The subscript 'o' stands for the initial value.

1.4 Finite Element Analysis

The main accomplishment during this reporting period involved the development of the general code. The main purpose of the general code is to reliably solve a large class of optimal control problems with a minimum of user-written subroutines. To this end, the general code runs on a SUN 3 and later workstations. It and requires a FORTRAN 77 compiler, MACSYMA [2], and the Harwell subroutine library [3]. The general procedure can be broken into three parts that must interface together. The first part is the FORTRAN code. This code contains all the subroutines necessary to solve any of the optimal control problems described above. However, if certain problems require table look-up routines (such as aerodynamic data for a rocket model), then these subroutines must be given by the user and interfaced to the rest of the general code. Thus, there may be a need for some user programming for certain problems. The second part of the general procedure is the use of MACSYMA. The user must supply an input file specifying the problem. This input file is in symbolic form and will be loaded into MACSYMA. MACSYMA will then evaluate all the necessary expressions and automatically generate the FORTRAN code. This code is spliced into a template file and becomes one of the subroutines. The third and final part of the general procedure will consists of subroutines to generate initial guesses that will reliably converge. A continuation method is being used which converts the algebraic equations to

initial-value ordinary differential equations. A second-order Runge-Kutta method is then used to integrate the equations and obtain initial guesses for a Newton-Raphson method. We also continued to further document the methodology through the publication of one paper [4] and the completion of three others. The first of these three is a technical note [5] which covers the extension of the method to state-control inequality constraints. The second deals with the application of the method to the ALS problem, per se [6]. Both of these are now accepted for publication. The third deals with the general code and will be presented at the upcoming ACC meeting [7].

2. Errata

An error in our previous 2-stage ALS optimal solution was found. The optimality condition was incorrectly formulated due to a missing conversion factor from degree to radian. The correct results are now shown in Figures 9 - 15. There are 3 jumps in the control profile (Figure 9). The first two jumps are due to the fact that the Hamiltonian is a non-convex function of the control. These jumps occur at about Mach 1.4 and 2.0 respectively. The last small jump is due to staging. However, the costates are all continuous. Though the control profile changes substantially, the performance index (final time) differs by less than 0.1s. Figures 16, 17 are the optimal solution under αq-constraint. The final time in this case is 362.103s which is 0.007s more than the unconstrained case.

3. Future Research

3.1 Analytical Investigation

We will follow two different directions. One will be the continuation of the modification of the regular perturbation technique. A first order closed loop simulation will be done. We will investigate the effect of number of segments and the segment intervals on the computational performance. At present a first order correction can be done in 0.5 to 7.0 CPUsec, depending on the current vehicle altitude on a MacIIci (a 32-bit 25MHz PC). At low altitude, the complicated aerodynamic effects require a more dense integration steps to complete the quadratures, however, the computational time can be significantly shortened if we perform parallel processing. The other line of research direction is to investigate the slow manifold approach to singular perturbation to a launch vehicle trajectory. Further approximation and analysis are expected.

3.2 Finite Elements Work

In the finite element analysis area we plan to continue to port the general code and complete a user's manual for it. We further plan to document the methodology through the completion of one paper (which we are now revising in response to reviewers) on the application of the method to launch vehicle trajectory analysis, two technical notes on control and state inequality constraints, one paper on the general code, and a user's manual for the code. We continue to receive calls from parties interested in application of the methodology in industry, and still hope to transfer the technology to an industry application in the future.

In a future phase of the work we hope to extend the work to higher-order finite element shape functions – the so-called p-version of the finite element method. This approach has been shown to be of value in linear time-domain problems [8] but has not yet been investigated for the nonlinear case.

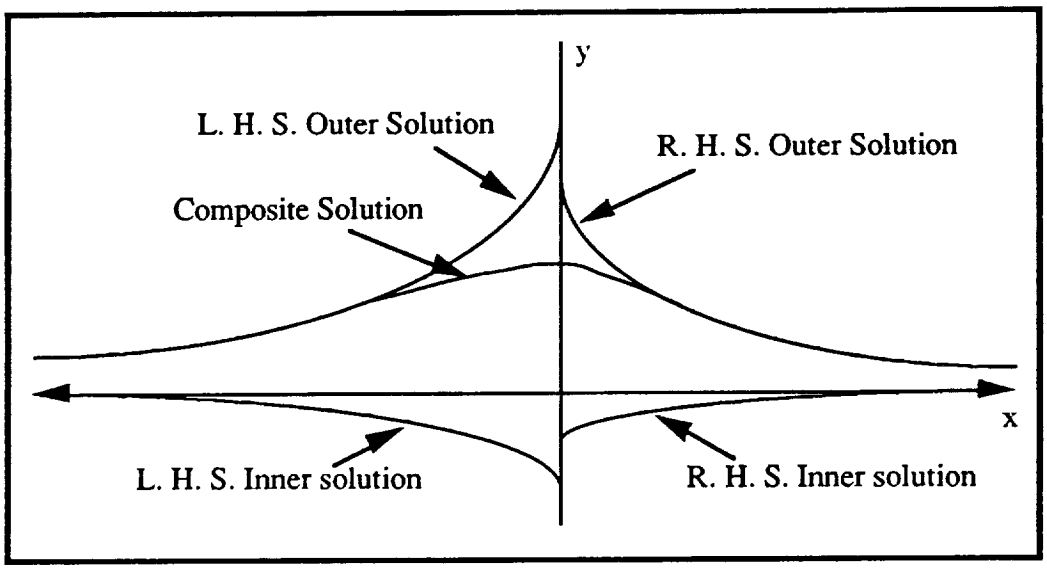

Figure 1. Illustration of Using MAE on the Launch Vehicle Problem

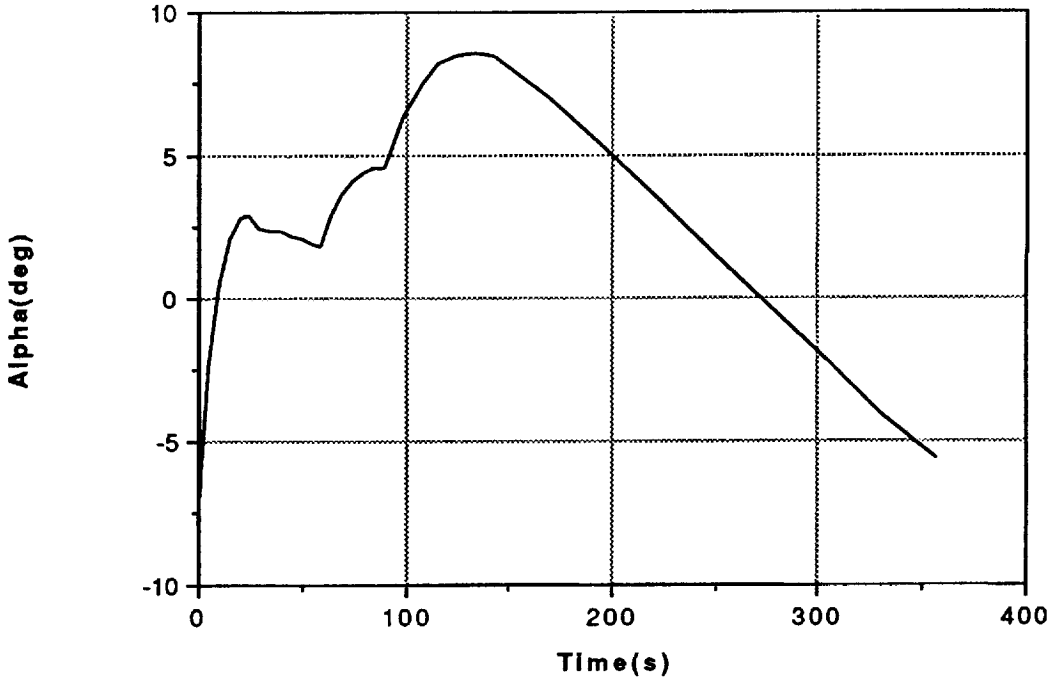

Figure 2. Angle of Attack Profile (4-pc. Zeroth Order Solution)

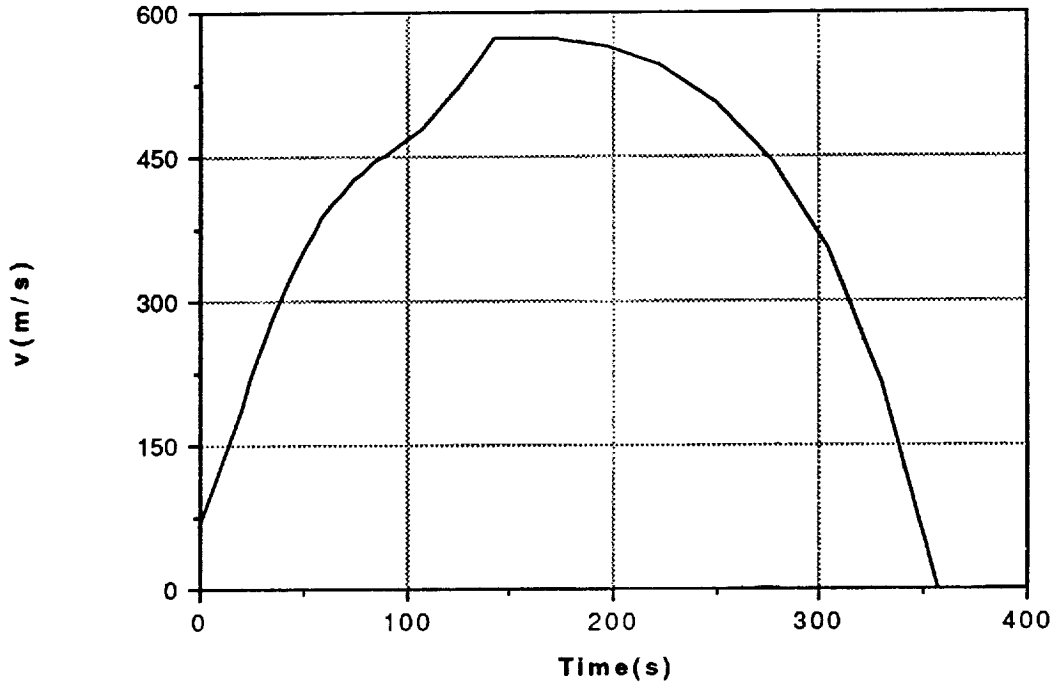

Figure 3. Vertical Velocity Component Profile

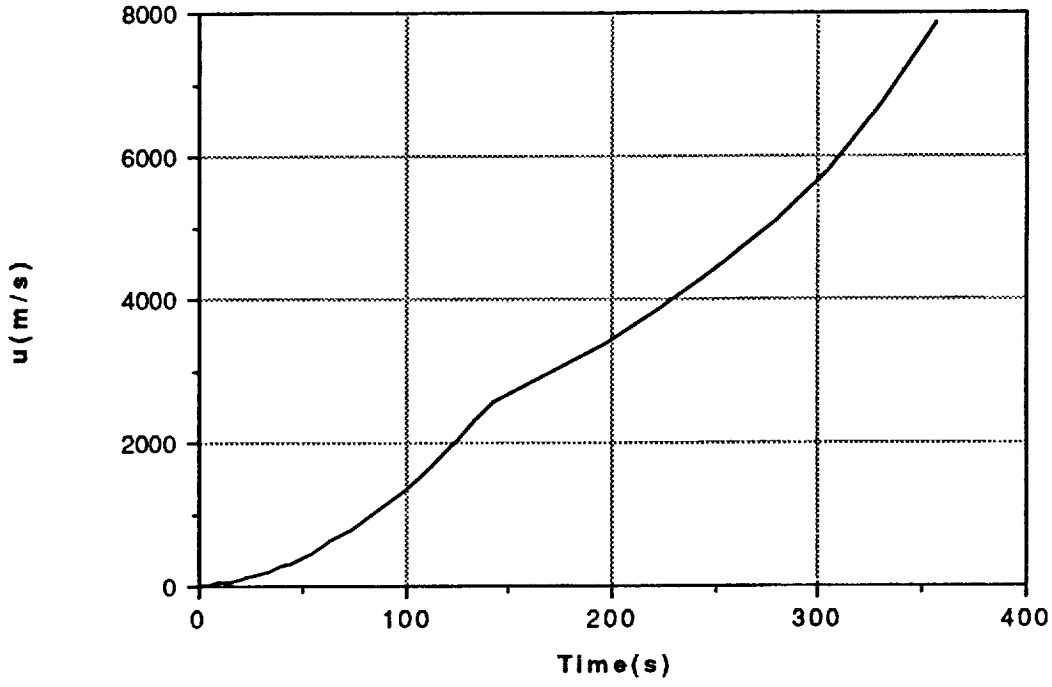

Figure 4. Horizontal Velocity Component Profile

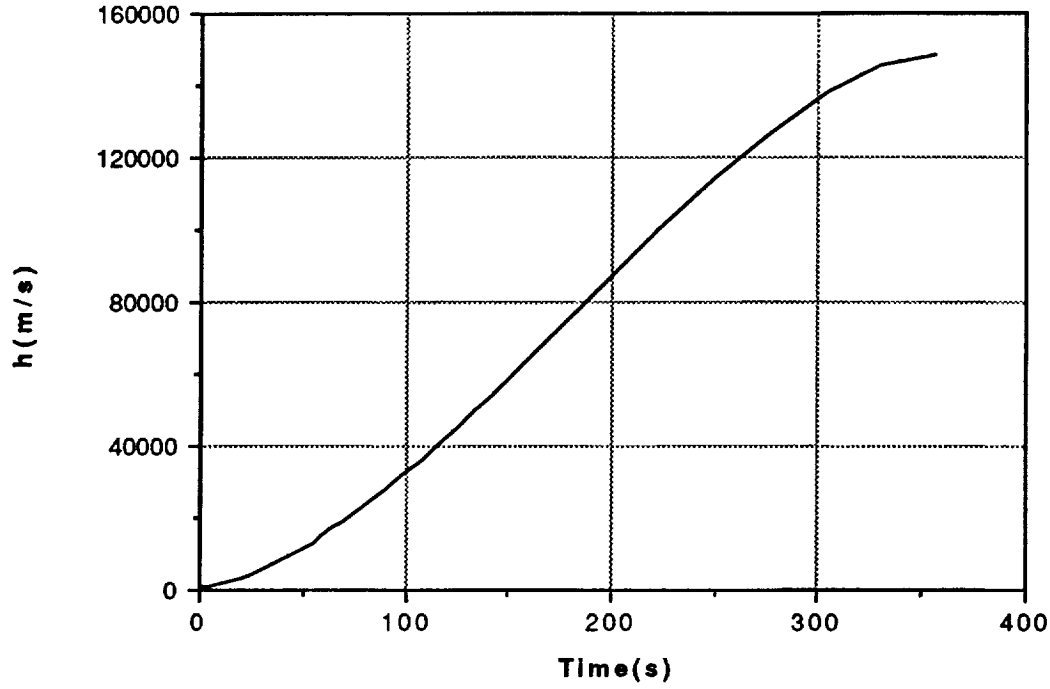

Figure 5. Altitude Profile

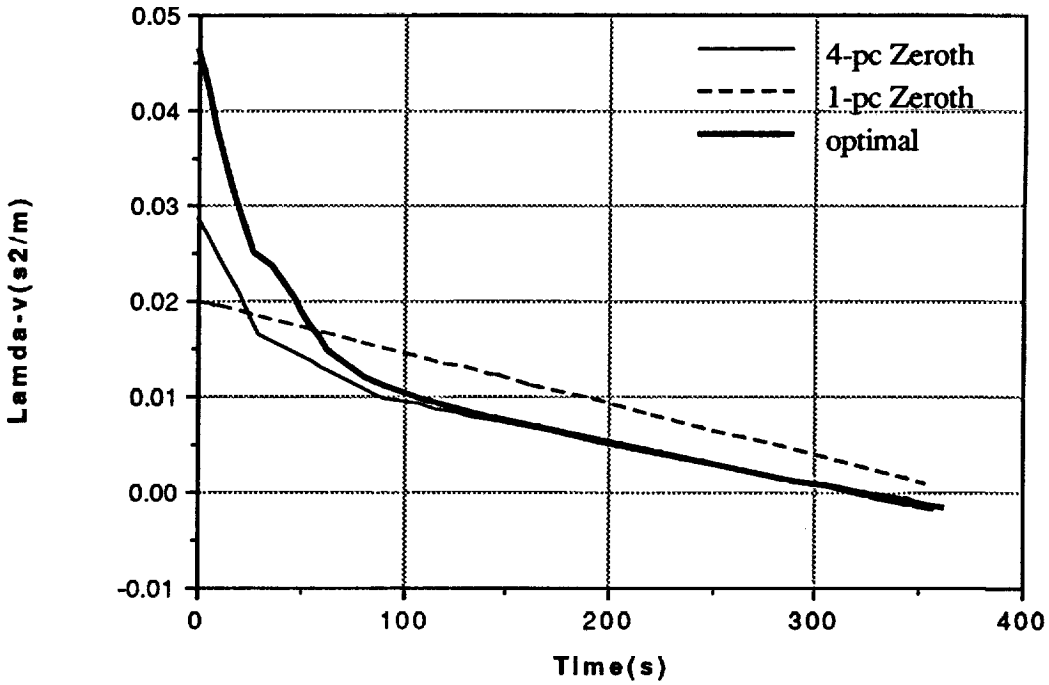

Figure 6. Vertical Velocity Component Costate Profile

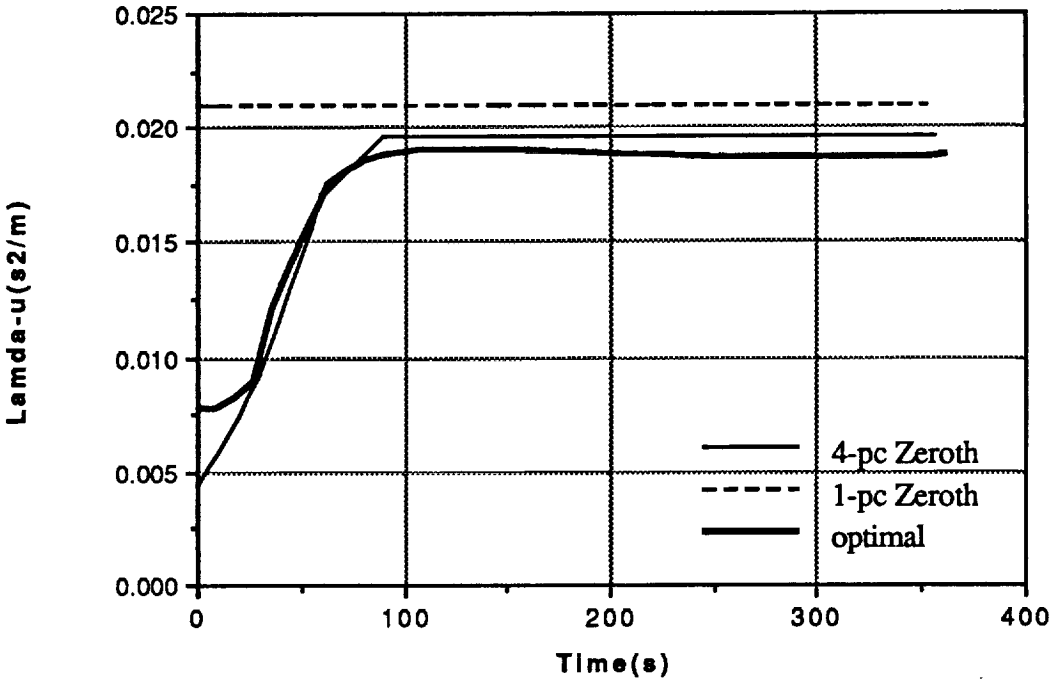

Figure 7. Horizontal Velocity Component Costate Profile

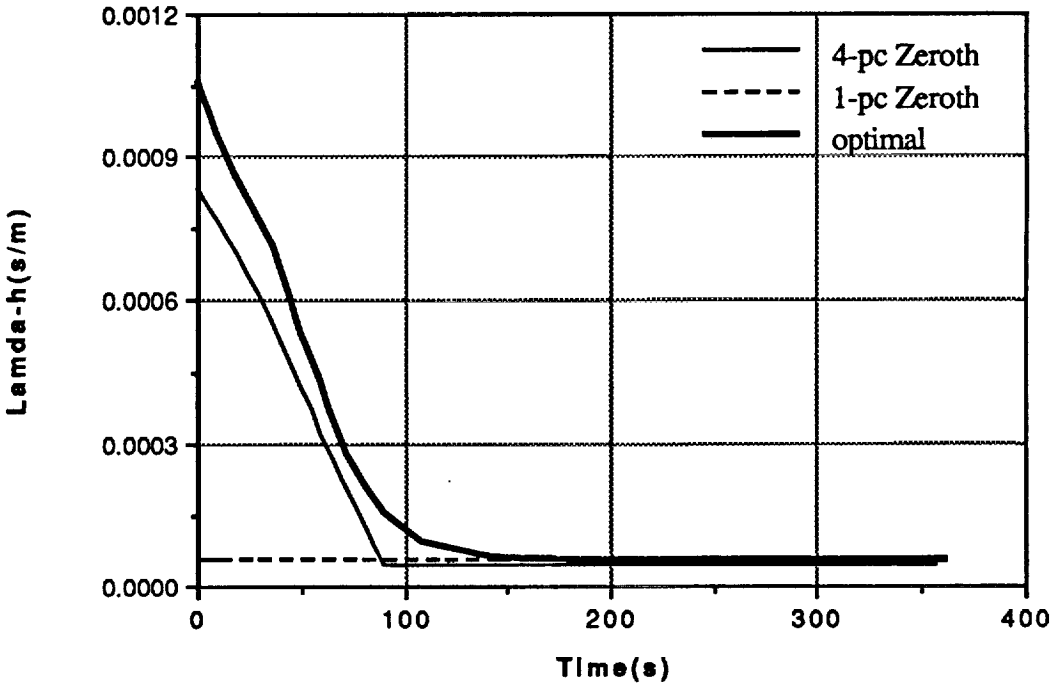

Figure 8. Altitude Costate Profile

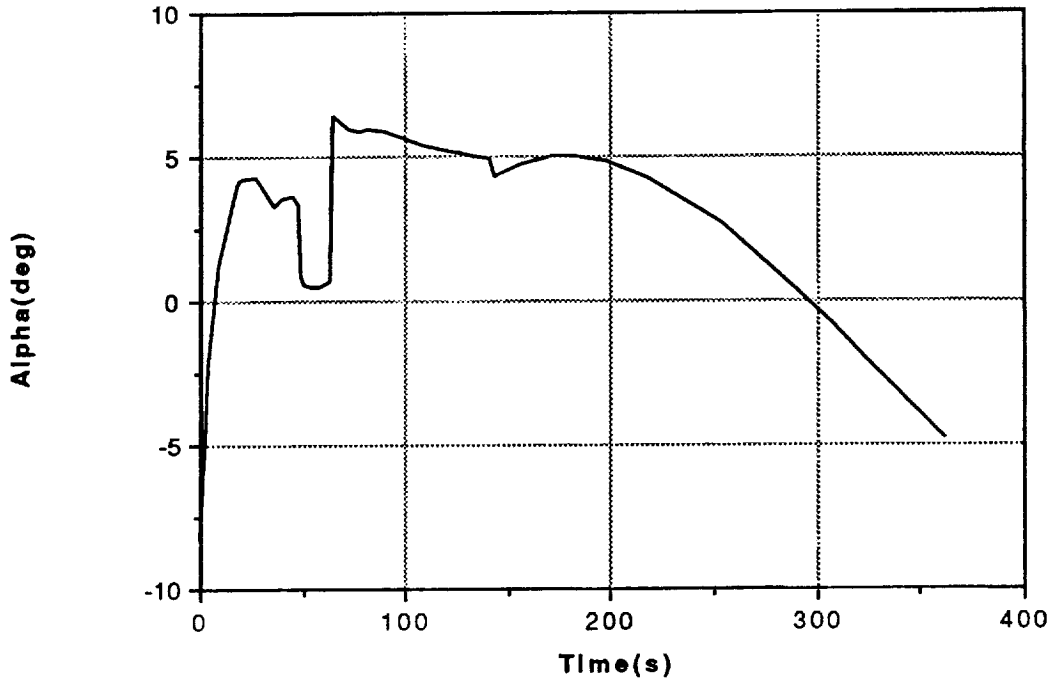

Figure 9. Optimal Angle of Attack Profile (Unconstrained Case)

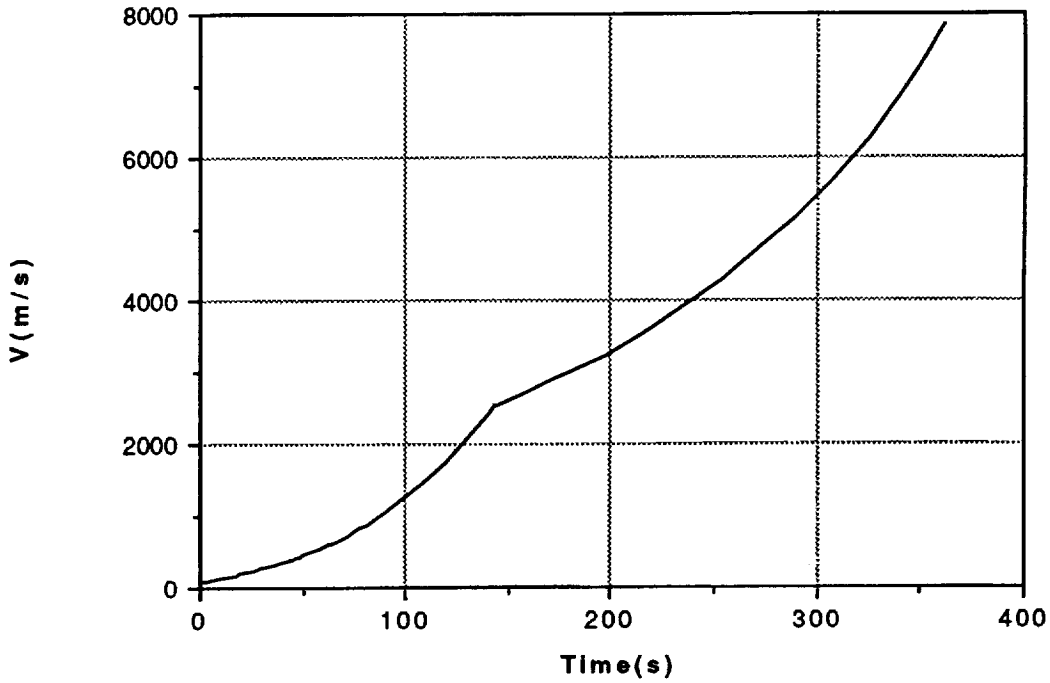

Figure 10. Velocity Profile

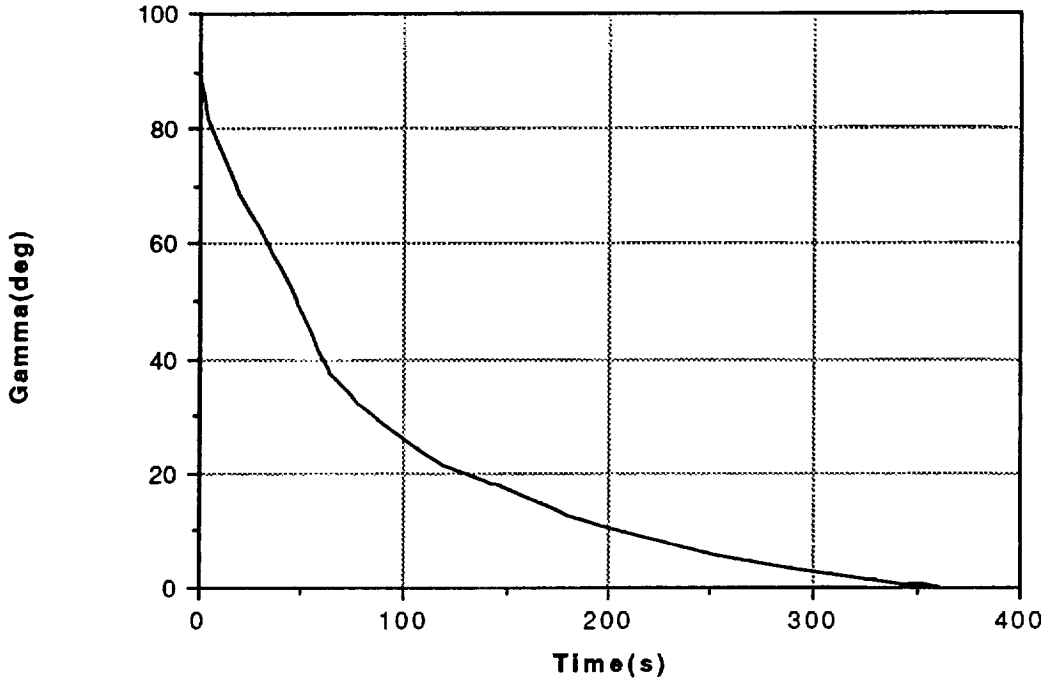

Figure 11. Flight Path Angle Profile

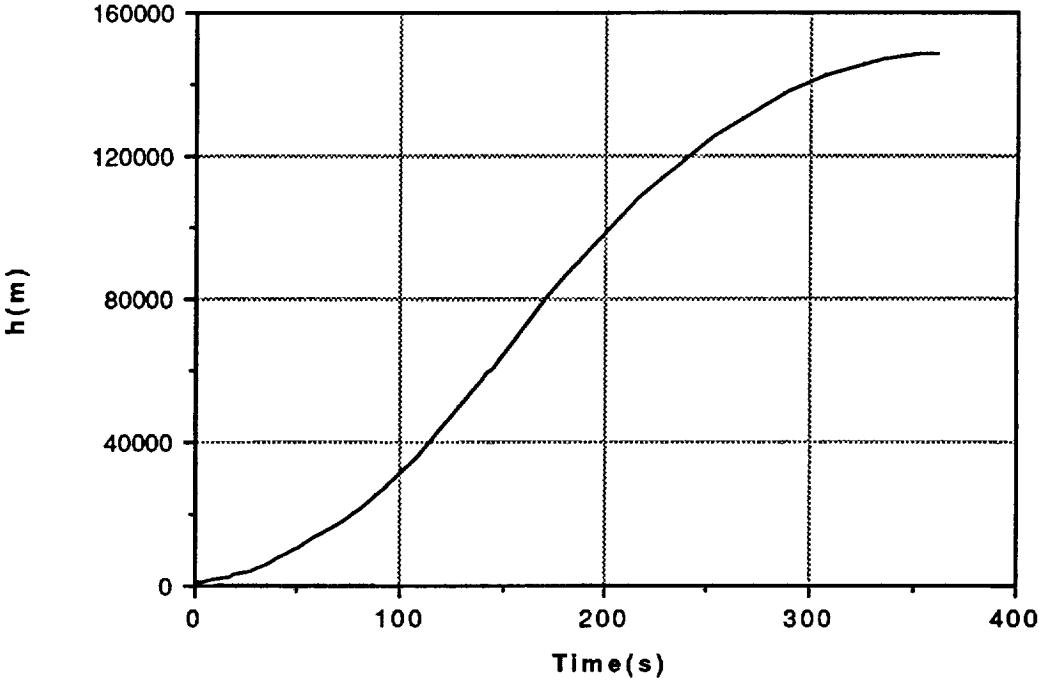

Figure 12. Altitude Profile

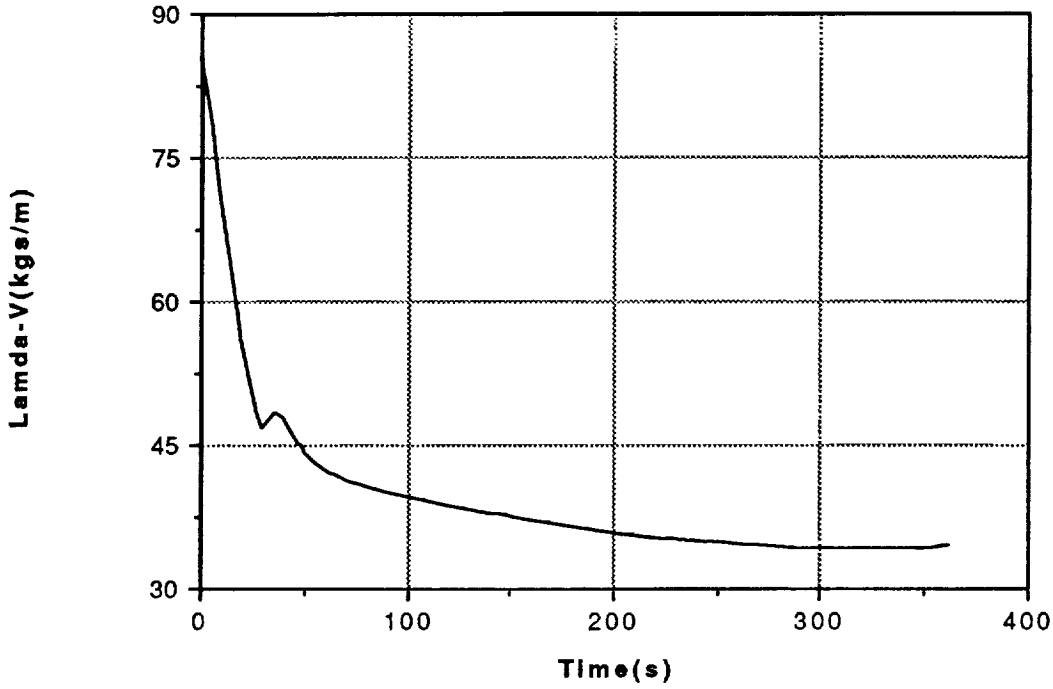

Figure 13. Velocity Costate Profile

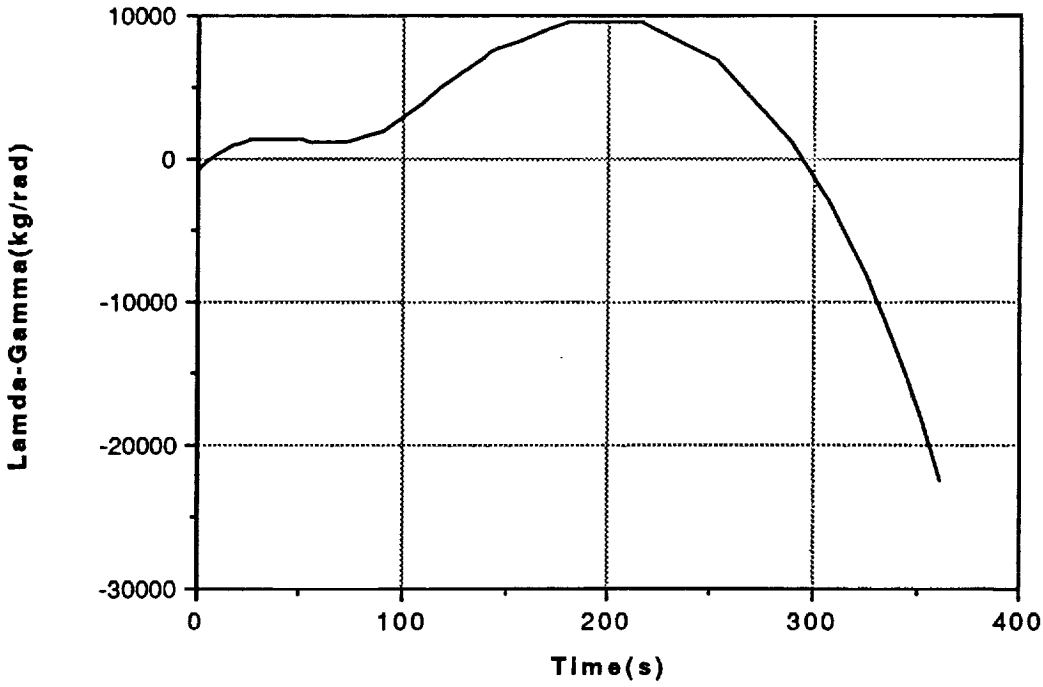

Figure 14. Flight Path Angle Costate Profile

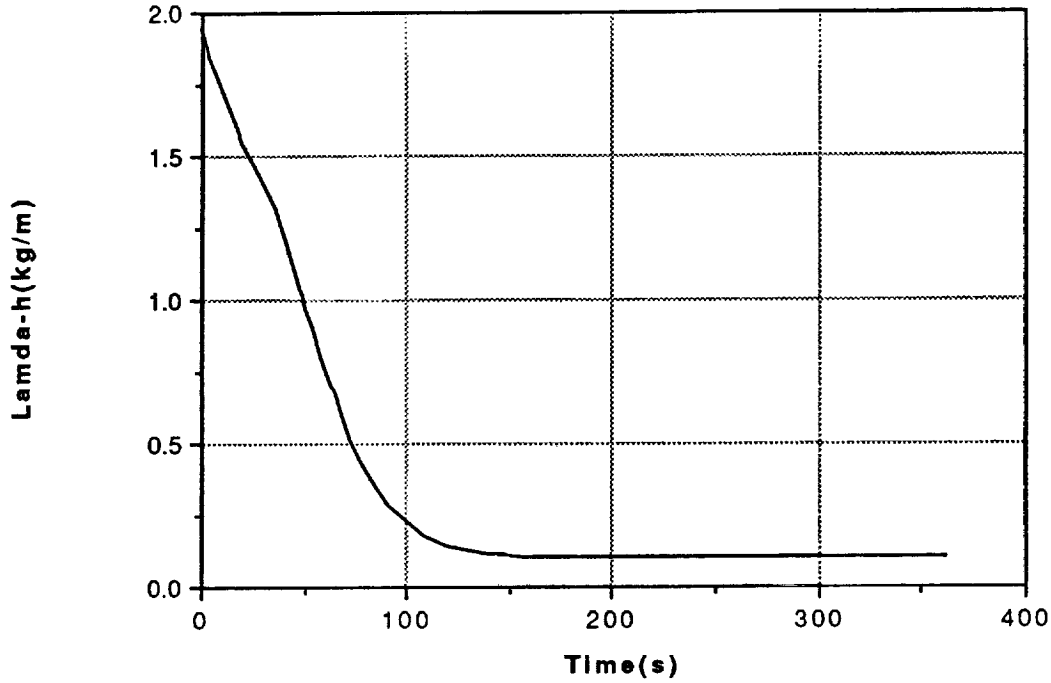

Figure 15. Altitude Costate Profile

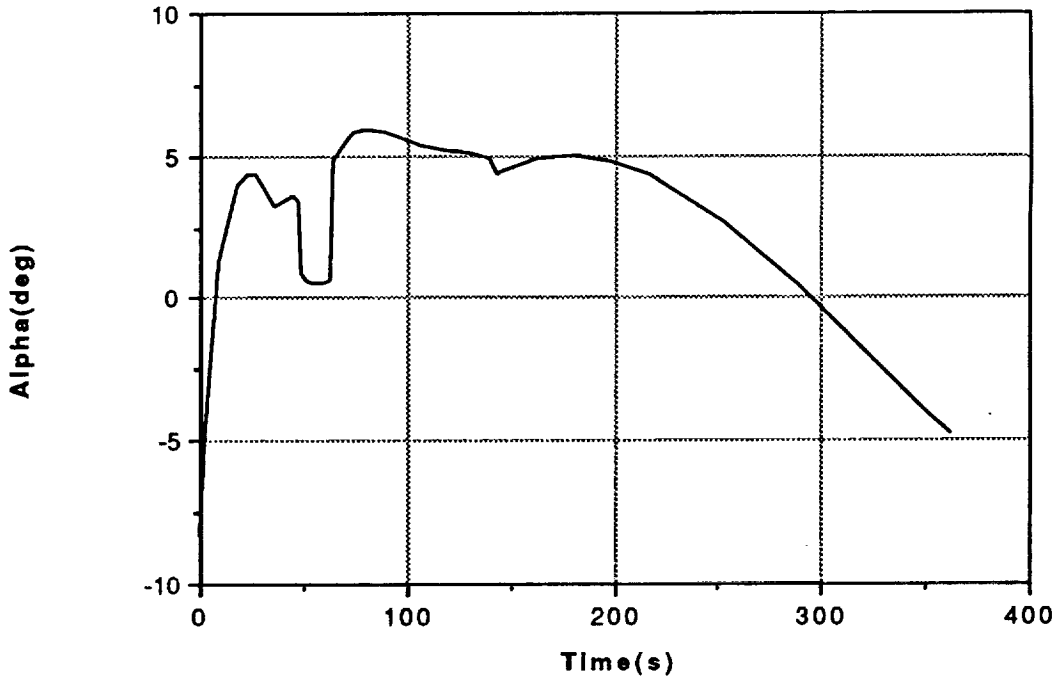

Figure 16. Optimal Angle of Attack Profile with αq-constraint

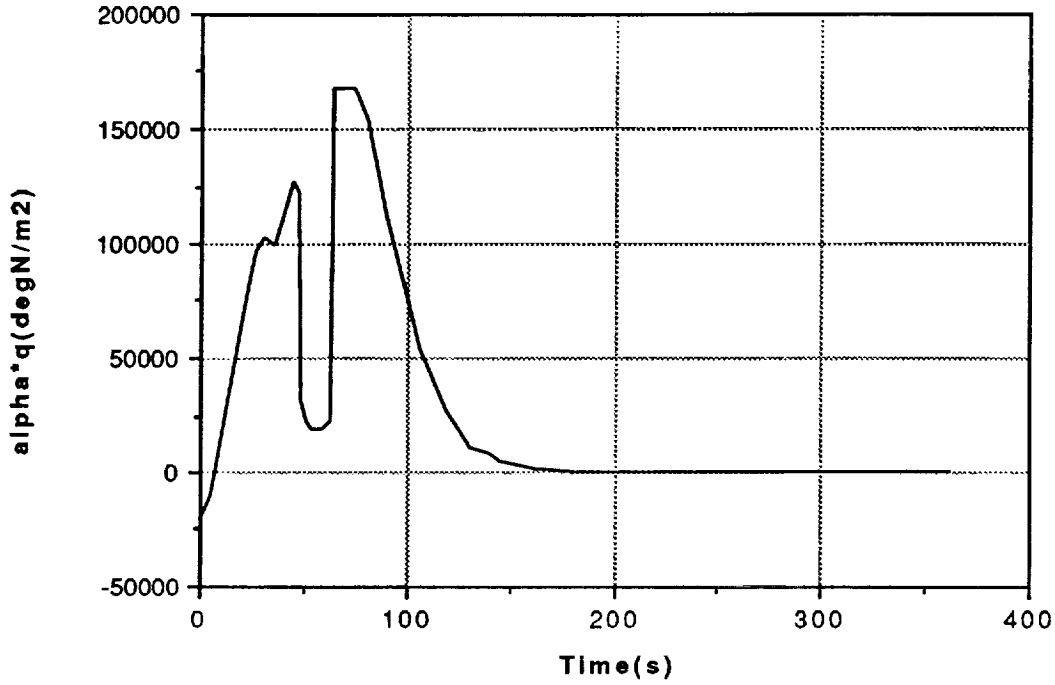

Figure 17. αq Profile of the Constrained Case

References

[1] Robert R. Bless, "Time-Domain Finite Elements in Optimal Control with Application to Launch-Vehicle Guidance," Ph.D. Dissertation, School of Aerospace Engineering, Georgia Institute of Technology, March 1991 (to be published as a NASA CR, 1991).

[2] MACSYMA Reference Manual, Symbolics, Inc., Burlington, Massachusetts, 1988.

[3] Duff, I. S., Harwell Subroutine Library, Computer Science and Systems Division Harwell Laboratory, Oxfordshire, England, February 1988, Chapt. M.

[4] Hodges, Dewey H., and Bless, Robert R., "A Weak Hamiltonian Finite Element Formulation for Optimal Control Problems," J. Guidance, Control, and Dynamics, vol. 14, no. 1, January-February 1991, pp. 148 – 156.

[5] Hodges, Dewey H., Calise, Anthony J., Bless, Robert R., and Leung, Martin, "Finite Element Method for Optimal Guidance of an Advanced Launch Vehicle," J. Guidance, Control, and Dynamics, to appear, 1991.

[6] Bless, Robert R., and Hodges, Dewey H., "Finite Element Solution of Optimal Control Problems with State-Control Inequality Constraints," J. Guidance, Control, and Dynamics, to appear, 1991.

[7] Bless, Robert R, and Hodges, Dewey H., "A Hybrid Symbolic/Finite-Element Algorithm for Solving Nonlinear Optimal Control Problems," Proceedings of the American Control Conference, Boston, Massachusetts, June 26 – 28, 1991, to appear.

[8] Hodges, Dewey H., and Hou, Lin Jun, "Shape Functions for Mixed p-Version Finite Elements in the Time Domain," J. Sound and Vibration, vol. 145, no. 2, March 8, 1991, pp. 169 – 178.

[9] Shi, Y. Y., "Matched Asymptotic Solutions For Optimum Lift Controlled Atmospheric Entry", AIAA Journal, Vol. 9, Nov. 1971, pp. 2229 - 2238.

[10] Ardema, M. D., "Singular Perturbations In Flight Mechanics", NASA TM X-62, 380, 1977.

[11] Calise, A. J., Melamed, N., "Analytical Guidance Law Development For Aerocapture at Mars", Progress Report, Dec. 90 - Apr. 91, NASA Grant # NAG-1-1139.

[12] Leung, S. K., Calise, A. J., "An Approach To Real-time Guidance Law For An Advanced Launch System", American Control Conference Proceedings, June 1990, San Diego,

[13] Hargraves, C. R., Paris, S. W., "Direct Trajectory Optimization Using Nonlinear Programming and Collocation", J. Guidance, Control and Dynamics, Vol. 10, July - Aug. 1987, pp. 338-342.

[14] Kokotovic, P. V., Khalil, H. K., O'Reilly, J., *Singular Perturbation Methods In Control: Analysis & Design*, Academic press, 1986.

[15] Calise, A. J., Hodges, D. H., Leung, S. K., Bless, R. R., "Optimal Guidance Law Development for an Advanced Launch System", Interim Progress Report, Dec. 90 - Jun. 91., NASA Grant # NAG-1-939.